machines

Communication

Highly Stretchable and Kirigami-Structured Strain Sensors with Long Silver Nanowires of High Aspect Ratio

Huiyan Huang [1,2], Catherine Jiayi Cai [2,3], Bok Seng Yeow [2], Jianyong Ouyang [4] and Hongliang Ren [2,5,*]

1 Hwa Chong Junior College, Singapore 269734, Singapore; ehuanghuiyan@gmail.com
2 Department of Biomedical Engineering, National University of Singapore, Singapore 117575, Singapore; caijiayi@u.nus.edu (C.J.C.); e0426370@u.nus.edu (B.S.Y.)
3 Singapore Institute of Manufacturing Technology, Singapore 138634, Singapore
4 Department of Materials Science and Engineering, National University of Singapore, Singapore 117575, Singapore; mseoj@nus.edu.sg
5 Department of Electronic Engineering, Faculty of Engineering, The Chinese University of Hong Kong, Hong Kong 999077, China
* Correspondence: ren@nus.edu.sg

Abstract: Stretchable, skin-interfaced, and wearable strain sensors have risen in recent years due to their wide-ranging potential applications in health-monitoring devices, human motion detection, and soft robots. High aspect ratio (AR) silver nanowires (AgNWs) have shown great potential in the flexible and stretchable strain sensors due to the high conductivity and flexibility of AgNW conductive networks. Hence, this work aims to fabricate highly stretchable, sensitive, and linear kirigami strain sensors with high AR AgNWs. The AgNW synthesis parameters and process windows have been identified by Taguchi's design of experiment and analysis. Long AgNWs with a high AR of 1556 have been grown at optimized synthesis parameters using the one-pot modified polyol method. Kirigami sensors were fabricated via full encapsulation of AgNWs with Ecoflex silicon rubber. Kirigami-patterned strain sensors with long AgNWs show high stretchability, moderate sensitivity, excellent linearity (R^2 = 0.99) up to 70% strain and can promptly detect finger movement without obvious hysteresis.

Keywords: strain sensor; flexible sensor; stretchable sensor; silver nanowire; piezoresistivity; human health monitoring

Citation: Huang, H.; Cai, C.J.; Yeow, B.S.; Ouyang, J.; Ren, H. Highly Stretchable and Kirigami-Structured Strain Sensors with Long Silver Nanowires of High Aspect Ratio. *Machines* **2021**, *9*, 186. https://doi.org/10.3390/machines9090186

Academic Editor: Dan Zhang

Received: 30 July 2021
Accepted: 27 August 2021
Published: 3 September 2021

1. Introduction

Stretchable and wearable strain sensors have grown to prominence in recent years due to their wide potential applications in flexible electronics, rehabilitation and personal health-monitoring devices, human motion detection, and soft robots [1,2]. Despite these sensors showing great promise in future health monitoring, more studies are needed to create a customizable yet scalable fabrication approach to improve the sensing properties. Herein, stretchability, sensitivity, and linearity are crucial for wearable strain sensors while ensuring excellent skin conformation for in situ health monitoring [3]. Recently, nanomaterials have received great interest in the development of strain sensors. Carbon nanomaterials such as graphene and carbon nanotubes have been used to fabricate strain sensors due to their superior mechanical and electrical properties. For example, graphene on flexible substrates has been used to fabricate high-sensitivity strain sensors [4,5]. However, these carbon-based strain sensors show low stretchability, non-linearity, and high hysteresis.

Silver nanowires (AgNWs) are one-dimensional silver nanostructures [6]. AgNWs have shown great potential in the fabrication of flexible and stretchable strain sensors due to the high conductivity and flexibility of AgNW conductive networks [7,8]. However, AgNWs embedded in the strain sensors shows surface buckling tendency, leading to permanent loss of contact between adjacent AgNWs [9]. Therefore, repeated stretching of the AgNW strain sensors results in inconsistent and irreversible spikes in resistance, leading to poor linearity. It is known that long AgNWs with a high aspect ratio (AR, AR = Length L/diameter D) can form better resilient conductive networks, which helps to solve the issue. However, the diameter and length of AgNWs reported in the literature are in the range of 10–200 nm and 5–100 µm, respectively, and most of the AR values are below 1000 [6].

Kirigami-like structures, originating from Chinese traditional paper-cutting art, are increasingly adopted as a new type of easily adjustable and deformable framework [10], which can be applied to a variety of stretchable devices, such as solar panels [11], smart adhesion devices [12], implantable and stretchable bio-probes [13], as well as tunable optical gratings [14]. These kirigami strain sensors can give linear and regular resistance change from the deformation of the created cut patterns from two to three dimensions [15]. This significantly reduces strain on the sensor material in high stretching conditions [16,17] and alleviates the surface buckling of the AgNW network under increasing strain, hence making the sensors more reliable.

In this work, a synergic approach combining long AgNWs conductive network and kirigami architecture is proposed to spontaneously improve the stretchability and linearity of the AgNW strain sensors. As a systematic approach to optimize the variables to maximize performance by decreasing variability due to noise, increasing production efficiency, the Taguchi method reduces the scale of experiments compared to the traditional factorial approach. It is thus used to optimize the synthesis parameters for long AgNWs with high AR. Then, the AgNWs with high AR are used to fabricate kirigami-structured strain sensors.

2. Experiments

2.1. Materials

Polyvinylpyrrolidone (PVP) and ethylene glycol (EG) were purchased from Sigma Aldrich. Silver nitrate ($AgNO_3$), sodium chloride (NaCl), and potassium bromide (KBr) were obtained from GCE Laboratory Chemicals. Ecoflex™ Silicone Rubber was obtained from Smooth-on.

2.2. Taguchi Design of Experiment

The process window for AgNW synthesis has to be determined to optimize the synthesis parameters further and synthesize high-quality long AgNWs with high AR. Taguchi design of experiment (DOE) is used to study the effects of synthesis parameters on the dimension of AgNWs. Based on the literature [6–9], halide additive concentration, molar ratio of Cl:Br, PVP concentration and growth temperature are the top four critical factors for AgNW growth. Therefore, Taguchi DOE with four factors and three levels was designed. The $AgNO_3$ concentration is kept constant at 0.02 M. Table 1 shows the selected four control factors, each with three widely spaced levels, which make up the L9 (3ˆ4) orthogonal array with a total of nine experiments.

Table 1. The Taguchi DOE with four factors at three levels.

Factors	Level 1	Level 2	Level 3
Cl^-:Br^- molar ratio	1:3	1:1	3:1
Total Halide concentration [Cl^- + Br^-], mM	0.3	0.6	1.2
PVP concentration [PVP], M	0.04	0.07	0.1
Temperature (°C)	140	150	160

2.3. Synthesis and Characterizations of AgNWs

The AgNWs were synthesized through a modified one-pot polyol method using $AgNO_3$ as a source of Ag, PVP as a capping agent, ethylene glycol as both a solvent and reducing agent, as well as halides as seeding additives. The adding amount of each chemical was referred to the L9 (3ˆ4) orthogonal array with a total of nine experiments in Table 2. First, PVP powders were dissolved in 100 mL EG solvent in a 150 mL glass bottle under magnetic stirring. Then, $AgNO_3$ was added to the PVP EG solution. After dissolving $AgNO_3$, respective volumes of 0.01 M NaCl and 0.01 M KBr EG solution were added to the PVP-$AgNO_3$ solution. Finally, the precursor was heated to the respective growth temperature for 4 h. The AgNW samples were cleaned with isopropanol (IPA) three times and then stored in IPA for usage. An optical microscope and scanning electron microscope (SEM) were used to observe the morphologies of the AgNWs. The lengths and diameters of the AgNWs were calculated by the ImageJ image processing program.

Table 2. Synthesis parameters and dimension of the AgNWs from Taguchi L9 (3ˆ4) orthogonal array.

Experiment No.	Cl^-:Br^- Molar Ratio	Halide Concentration: $[Cl^- + Br^-]$ (mM)	PVP Concentration: [PVP] (M)	Temperature (°C)	AgNW Diameter, D (nm)	AgNW Length, L (μm)
#1	1:3	0.3	0.04	140	97.3	0
#2	1:3	0.6	0.07	150	44.1	16.3
#3	1:3	1.2	0.10	160	22.3	10.9
#4	1:1	0.3	0.10	150	71.9	0
#5	1:1	0.6	0.04	160	36.4	20.7
#6	1:1	1.2	0.07	140	62.1	15.7
#7	3:1	0.3	0.07	160	19.3	0
#8	3:1	0.6	0.10	140	69.1	10.7
#9	3:1	1.2	0.04	150	28.7	29.5

2.4. Fabrication of Kirigami Strain Sensor

The fabrication processes of the kirigami-structured strain sensors with AgNWs are illustrated in Figure 1. First, AgNW IPA suspension was poured onto a filter paper and a thin uniform AgNW film was obtained through vacuum filtration. The thickness and transparency of the AgNW film can be controlled by varying the concentration and volume of the AgNW IPA suspension used during vacuum filtration. Second, the AgNW film on filter paper was then patterned using a Silhouette Curio machine. Third, the Ecoflex precursor was spin-coated onto the patterned AgNW film as a stretchable substrate. After the Ecoflex cures, the AgNW-Ecoflex composite was then detached from the underlying filter paper. The AgNW-Ecoflex composite was then cut into small rectangle strips. Finally, the copper tape was secured on both ends of the AgNW film with silver paste to form the external connections of the strain sensor.

The gauge factor (GF) of the strain sensor relative to its strain is compared by measuring its percentage change in length with a vernier caliper and the consequent resistance change of the sensor with a multimeter. The AgNW strain sensors are then mounted onto the fingers, and real-time detection of strain is achieved by connecting the sensor to an Arduino and measuring the resistance change of the sensor in relation to the bending degree of the sensor finger.

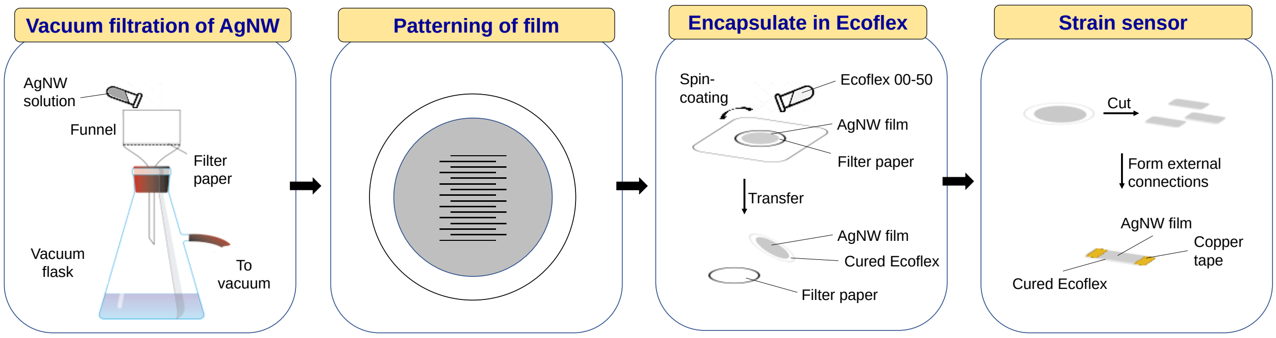

Figure 1. Fabrication processes of the kirigami-structured strain sensor with AgNWs. With regards to the network structure of AgNWs, the kirigami patterning was done on the AgNW film before spin-coating Eco-Flex on the network. This patterning also significantly decreases the hysteresis of the strain sensor, showing this architecture improved the conductive network of the AgNWs.

3. Results and Analysis

The length and diameter of AgNWs synthesized in the nine experiments of Taguchi DOE are listed in Table 2. Due to the wide variation of the synthesis parameters, the samples vary from Ag nanoparticles ($L = 0$) to AgNWs with D = 28.7–97.3 nm and L = 10.7–29.5 µm. Among all nine experiments, Sample #9 produced long AgNWs with the highest AR = 1028.

The significance analysis is used to determine how four individual synthesis factors affect the length and diameter of the AgNWs. As shown in Figure 2a, the AgNW length increases continuously with increasing Cl:Br ratio and the concentration of halide and PVP, while decreases with increasing growth temperature. Figure 2b shows that the AgNW diameter decreases with increasing Cl:Br ratio, the concentration of halide, and PVP. However, with a further decrease of the growth temperature below 140 °C, only silver nanoparticles were obtained and no AgNWs can be synthesized. At lower temperatures below 140 °C, the reducing power of EG is significantly decreased. Therefore, the Ag^+ could not be driven to selectively bind on the {111} facet, causing isotropic growth and thus forming Ag nanocrystals rather than AgNWs at lower temperatures [18]. To promote the anisotropic growth of AgNWs, Ag^+ must be reduced and driven to accumulate on the {111} faces located on both ends, resulting in growth along both ends and resulting in anisotropic growth along {110}. At moderately high temperatures above 140 °C, the driving force for the formation of AgNWs shifts to the reduction of Ag^+ ions by EG, resulting in the greater formation of Ag nuclei. This initially leads to mild growth of ultra-long AgNWs up to 168 µm at 140 °C. However, with increasing growth temperature further to 160 °C, more Ag nuclei are formed. The growth rate is faster due to the high Ag^+ ions reduction rate, which consumes many Ag^+ ions resources and thus results in short AgNWs with large diameters mixed with Ag nanocrystals.

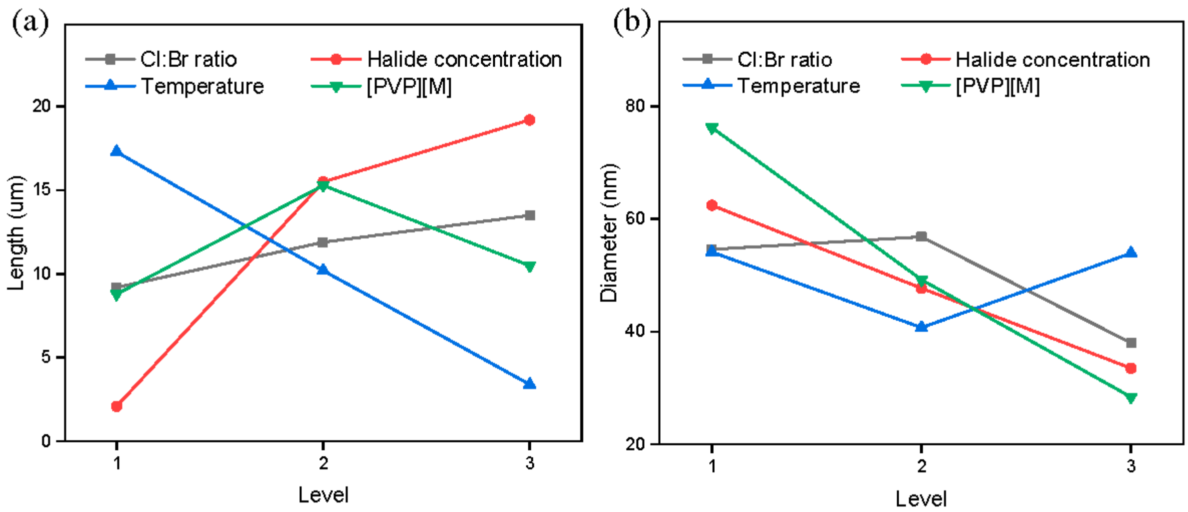

Figure 2. Significance analysis of the effects of the four synthesis parameters with three-level variations on (**a**) length and (**b**) diameter of AgNWs synthesized by Taguchi DOE in Table 2.

Based on "the higher, the better" criteria for length and "the smaller, the better" criteria for diameter, the optimal parameters obtained from significance analysis (Figure 2) to synthesize long AgNWs with high AR (small diameter) are: Cl:Br ratio = 3:1, halide concentration = 1.2 mM, [PVP] = 0.07–0.1 M, temperature = 140–150 °C. Therefore, the optimal synthesis parameters were used to synthesize AgNWs for verification. As shown in Figure 3a,b, the synthesized AgNWs are very uniform in dimension with high purity. The length distribution of the AgNWs ranges from 60 µm to 180 µm (Figure 3c), and the average mean length is 112 µm. The diameter of the AgNWs is in the range of 20 nm to 140 nm, with a mean diameter of 72 nm (Figure 3d). The AR calculated from the mean L/D is 1556, which is 1.5 times the best Taguchi Sample #9. The results confirm that the length and AR of AgNWs can be further improved by optimizing synthesis parameters through Taguchi DOE. The AR value reported in the literature is summarized in Figure 3e. Most of the reported AR value is below 1000, typically at around 600 [6]. Before parameter optimization, the best AR = 1028 obtained from Taguchi Sample #9 is higher/comparable with those reported AR values. Furthermore, after optimizing the synthesis parameter, the AR increases remarkably to 1556, which is much higher than those reported AR value.

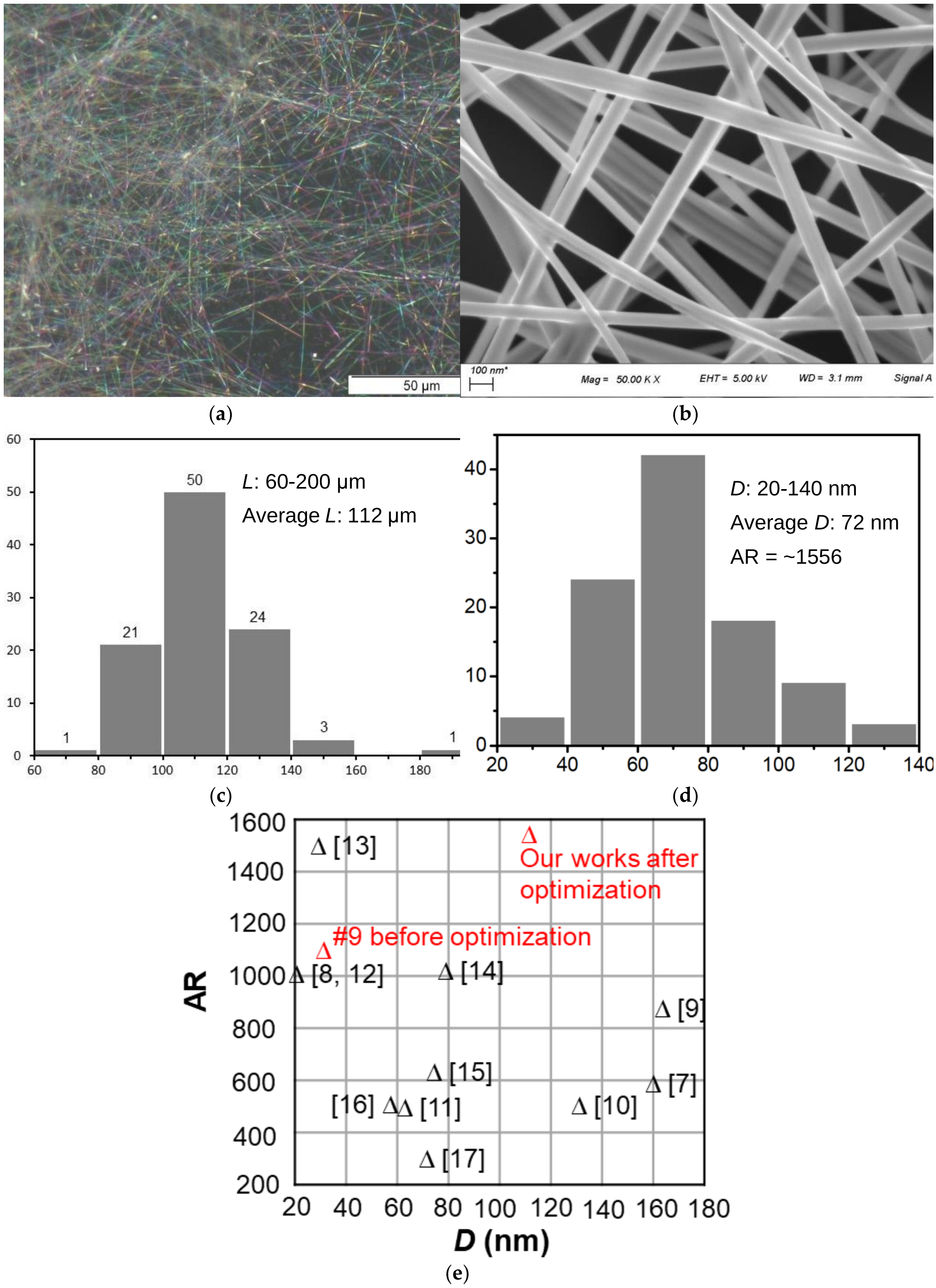

Figure 3. (**a**) Optical microscope and (**b**) Scanning Electron Microsopy images of the AgNW, (**c**) length and (**d**) diameter distribution of AgNWs synthesized at optimized synthesis conditions; (**e**) comparison of the AgNW AR of our works with other reported values of AgNW AR. It is necessary to emphasize that these AgNWs are those synthesized from the optimized batch, to distinguish themselves from the previous AgNWs synthesized as part of the Taguchi Design of Experiment, which also has AgNW diameter and length mentioned.

The strain sensors with and without kirigami patterning were successfully fabricated with AgNW electrodes. The strain sensing performance of the non-kirigami and kirigami patterned strain sensors are shown in Figure 4a,b, respectively. The non-kirigami strain sensors offer a lower stretchability and linearity with an R^2 value of 0.98 up to 25% strain (Figure 4a). The non-kirigami strain sensors have a GF ~6 but tend to crack at higher strain. On the other hand, the kirigami-structured strain sensors with long AgNWs show high stretchability and excellent linearity (R^2 ~ 0.99) up to 70% strain and good sensitivity (GF ~1.6). Furthermore, the kirigami-structured strain sensor shows no cracking after strain testing. As shown in Figure 4c, long AgNWs with high AR exhibited a greater tendency to curve in the conductive network. These curved silver nanowires straighten the resilience of the AgNW networks (Figure 4d), allowing the strain sensor to maintain AgNW conductive networks even at high strains, hence producing higher stretchability and linearity. Furthermore, kirigami patterns allow out-of-plane deformations of the strain sensor, thus increasing its stretchability and resistance to cracking but slightly compromising its sensitivity. In contrast with conventional strain sensors (GF ~ 2 with maximum stretchability of 5% and linear response), Carbon nanotube (CNT)/polymer composite (GF ~ 0.82 with stretchability of 40% and linear response) [19], graphene/polymer composite (GF > 1000 with stretchability of 5% and nonlinear response) [4], and carbon black/polymer composite (GF ~ 20 with stretchability of 80% but nonlinear response) [20], our strain sensors with long AgNWs outperform most of the strain sensors mentioned above by offering high sensitivity, stretchability, and linearity simultaneously.

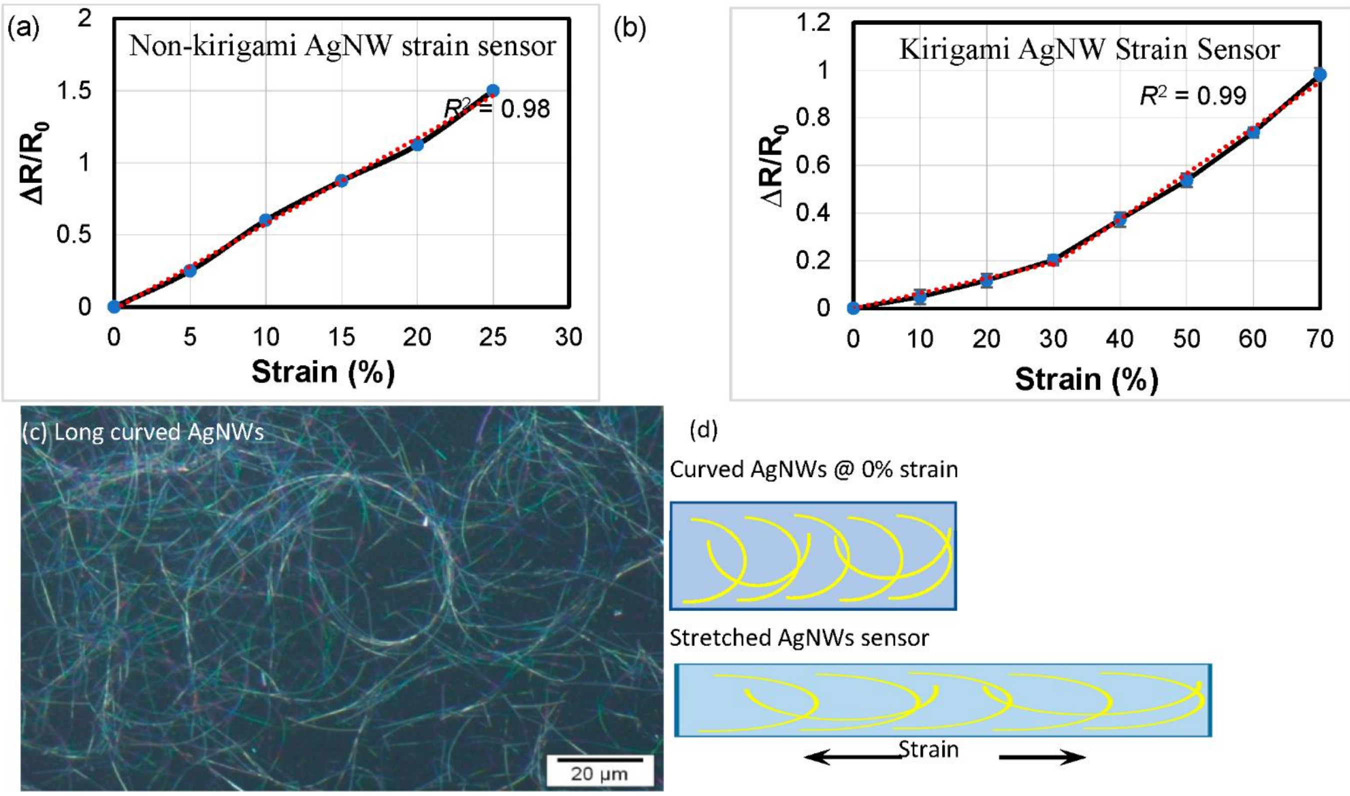

Figure 4. Response of (**a**) non-kirigami and (**b**) kirigami patterned sensors to strains; (**c**) Microscope image of the long curved AgNWs in the strain sensor; (**d**) Illustration of long curved AgNWs with high AR response to the strain.

Upon successful fabrication of AgNW strain sensors, the kirigami strain sensors were mounted on the glove's fingers, and successive bending tests were conducted (Figure 5a). The bending of the forefinger results in a sharp spike of the signal, while relaxing the forefinger decreases it. The AgNW strain sensors provide a coordinated signal response to a similar angular change of the fingers. Results obtained were consistent, showing immediate signal change and no noticeable hysteresis after repeated bending of the fingers at high frequency, proving its reliability after repeated bending cycles. Due to the large signal spike, data noise is negligible, leading to almost perfect peaks upon application of strain (Figure 5b). This further proves the sensor's application as a wearable strain sensor or personal health-monitoring devices and human motion detection.

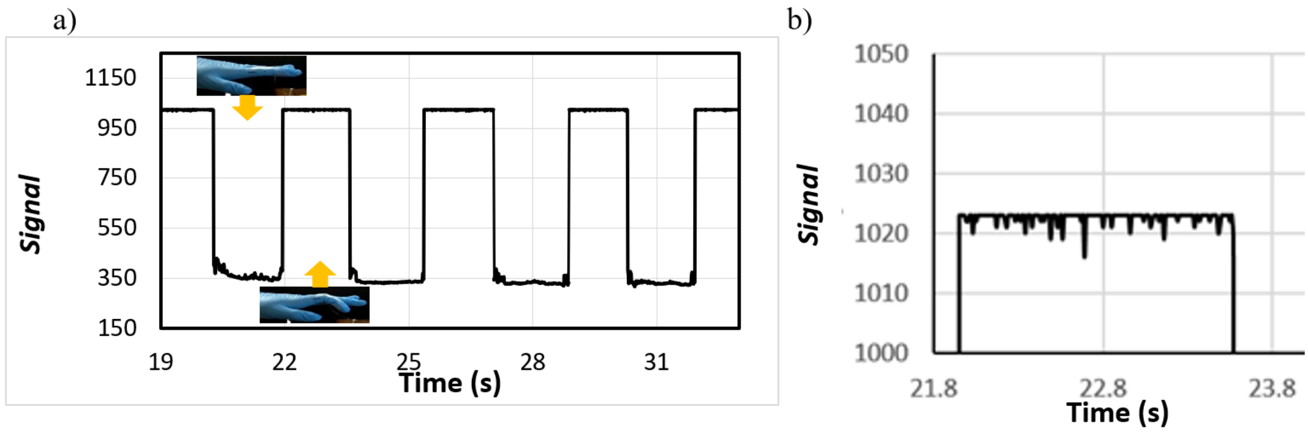

Figure 5. AgNW strain sensor response to finger bending movement for (**a**) five cycles and (**b**) a specific cycle.

4. Conclusions

AgNW synthesis parameters have been optimized by Taguchi's design of experiments. Long AgNWs up to 200 µm with a high average aspect ratio of 1556 have been synthesized with optimized synthesis parameters. Kirigami-patterned strain sensors with long AgNWs show high stretchability, moderate sensitivity, and excellent linearity (R^2 = 0.99) up to 70% strain. These strain sensors were mounted on the fingers, and the strain was measured in real-time to detect finger bending. The AgNW strain sensors can promptly detect finger movements without obvious hysteresis, finding wide applications in body movement and human health monitoring. The silver-nanowire conductive network itself is not a kirigami network. However, the term kirigami was nevertheless used as the final strain sensor was kirigami-patterned, as the kirigami patterning process in fabricating the AgNW sensor changes the conductive network of the AgNWs. This change in the percolation network due to the kirigami structure is shown from the lower hysteresis of the kirigami-structured AgNW sensor as compared to the non-kirigami patterned AgNW sensor.

Author Contributions: Conceptualization, H.H.; H.R.; J.O.; B.S.Y. and C.J.C.; methodology, H.H., C.J.C. and B.S.Y.; validation, J.O. and H.R.; formal analysis, H.H., B.S.Y. and C.J.C.; investigation, H.H., B.S.Y. and C.J.C.; resources, H.R.; data curation, H.H., C.J.C. and B.S.Y.; writing—original draft preparation, H.H.; writing—review and editing, H.R., J.O., C.J.C. and B.S.Y.; visualization, C.J.C. and H.H.; supervision, H.R.; project administration, H.R.; funding acquisition, H.R. All authors have read and agreed to the published version of the manuscript.

Funding: Singapore Academic Research Fund under Grant R397000353114.

Institutional Review Board Statement: Not applicable.

Informed Consent Statement: Not applicable.

Data Availability Statement: The data presented in this study are available on request from the corresponding author.

Conflicts of Interest: The authors declare no conflict of interest.

References

1. Amjadi, M.; Kyung, K.-U.; Park, I.; Sitti, M. Stretchable, skin-mountable, and wearable strain sensors and their potential applications: A review. *Adv. Funct. Mater.* **2016**, *26*, 1678–1698. [CrossRef]
2. Pegan, J.D.; Zhang, J.; Chu, M.; Nguyen, T.; Park, S.-J.; Paul, A.; Kim, J.; Bachman, M.; Khine, M. Skin-mountable stretch sensor for wearable health monitoring. *Nanoscale* **2016**, *8*, 17295–17303. [CrossRef] [PubMed]
3. Xi, W.; Yeo, J.C.; Yu, L.; Zhang, S.; Lim, C.T. Ultrathin and wearable microtubular epidermal sensor for real-time physiological pulse monitoring. *Adv. Mater. Technol.* **2017**, *2*, 1700016. [CrossRef]
4. Li, X.; Zhang, R.; Yu, W.; Wang, K.; Wei, J.; Wu, D.; Cao, A.; Li, Z.; Cheng, Y.; Zheng, Q.; et al. Stretchable and highly sensitive graphene-on-polymer strain sensors. *Sci. Rep.* **2012**, *2*. [CrossRef] [PubMed]
5. Hempel, M.; Nezich, D.; Kong, J.; Hofmann, M. A novel class of strain gauges based on layered percolative films of 2D materials. *Nano Lett.* **2012**, *12*, 5714–5718. [CrossRef] [PubMed]
6. Zhang, K.; Du, Y.; Chen, S. Sub 30 nm silver nanowire synthesized using KBr as co-nucleant through one-pot polyol method for optoelectronic applications. *Org. Electron.* **2015**, *26*, 380–385. [CrossRef]
7. Mutiso, R.M.; Sherrott, M.C.; Rathmell, A.R.; Wiley, B.; Winey, K.I. Integrating simulations and experiments to predict sheet resistance and optical transmittance in nanowire films for transparent conductors. *ACS Nano* **2013**, *7*, 7654–7663. [CrossRef] [PubMed]
8. Krantz, J.; Stubhan, T.; Richter, M.; Spallek, S.; Litzov, I.; Matt, G.J.; Spiecker, E.; Brabec, C.J. Spray-coated silver nanowires as top electrode layer in semitransparent P3HT:PCBM-based organic solar cell devices. *Adv. Funct. Mater.* **2012**, *23*, 1711–1717. [CrossRef]
9. Amjadi, M.; Pichitpajongkit, A.; Lee, S.; Ryu, S.; Park, I. Highly stretchable and sensitive strain sensor based on silver nanowire–elastomer nanocomposite. *ACS Nano* **2014**, *8*, 5154–5163. [CrossRef] [PubMed]
10. Sun, R.; Zhang, B.; Yang, L.; Zhang, W.; Farrow, I.; Scarpa, F.; Rossiter, J. Kirigami stretchable strain sensors with enhanced piezoelectricity induced by topological electrodes. *Appl. Phys. Lett.* **2018**, *112*, 251904. [CrossRef]
11. Lamoureux, A.; Lee, K.; Shlian, M.; Forrest, S.R.; Shtein, M. Dynamic kirigami structures for integrated solar tracking. *Nat. Commun.* **2015**, *6*. [CrossRef] [PubMed]
12. Hwang, D.-G.; Trent, K.; Bartlett, M.D. Kirigami-inspired structures for smart adhesion. *ACS Appl. Mater. Interfaces* **2018**, *10*, 6747–6754. [CrossRef] [PubMed]
13. Morikawa, Y.; Yamagiwa, S.; Sawahata, H.; Numano, R.; Koida, K.; Ishida, M.; Kawano, T. Flexible devices: Ultrastretchable kirigami bioprobes. *Adv. Heal. Mater.* **2018**, *7*, 1870017. [CrossRef]
14. Zhang, Y.; Yan, Z.; Nan, K.; Xiao, D.; Liu, Y.; Luan, H.; Fu, H.; Wang, X.; Yang, Q.; Wang, J.; et al. A mechanically driven form of Kirigami as a route to 3D mesostructures in micro/nanomembranes. *Proc. Natl. Acad. Sci. USA* **2015**, *112*, 11757–11764. [CrossRef]
15. Xu, K.; Lu, Y.; Honda, S.; Arie, T.; Akita, S.; Takei, K. Highly stable kirigami-structured stretchable strain sensors for perdurable wearable electronics. *J. Mater. Chem. C* **2019**, *7*, 9609–9617. [CrossRef]
16. Guan, Y.-S.; Zhang, Z.; Tang, Y.; Yin, J.; Ren, S. Kirigami-inspired nanoconfined polymer conducting nanosheets with 2000% stretchability. *Adv. Mater.* **2018**, *30*, e1706390. [CrossRef] [PubMed]
17. Yong, K.; De, S.; Hsieh, E.Y.; Leem, J.; Aluru, N.; Nam, S. Kirigami-inspired strain-insensitive sensors based on atomically-thin materials. *Mater. Today* **2019**, *34*, 58–65. [CrossRef]
18. Sun, Y.; Yin, Y.; Mayers, B.T.; Herricks, T.; Xia, Y. Uniform silver nanowires synthesis by reducing $AgNO_3$ with ethylene glycol in the presence of seeds and Poly(Vinyl Pyrrolidone). *Chem. Mater.* **2002**, *14*, 4736–4745. [CrossRef]
19. Yamada, T.; Hayamizu, Y.; Yamamoto, Y.; Yomogida, Y.; Izadi-Najafabadi, A.; Futaba, D.; Hata, K. A stretchable carbon nanotube strain sensor for human-motion detection. *Nat. Nanotechnol.* **2011**, *6*, 296–301. [CrossRef] [PubMed]
20. Jinhwan, L.; Lee, P.; Lee, H.; Lee, D.; Lee, S.S.; Ko, S.H. Very long Ag nanowire synthesis and its application in a highly transparent, conductive and flexible metal electrode touch panel. *Nanoscale* **2012**, *4*, 6408–6414.